September 2024, Vol:2, Issue:2

International Journal of New Findings in Engineering, Science and Technology

journal homepage: *https://ijonfest.gedik.edu.tr/*

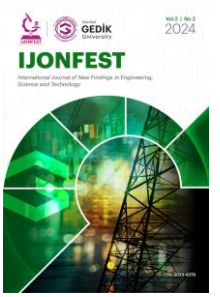

IMPLEMENTING THE STREAMLINE CURVATURE METHOD FOR PRELIMINARY DESIGN OF MULTISTAGE AXIAL COMPRESSORS

Rafis Mukhamediarov [a*], Hadi Genceli [a]

[a] *Department of Mechanical Engineering, Yildiz Technical University, Istanbul, Turkey,*
[*] *Corresponding author's email address: RafisMukhamedyarov@gmail.com*

Abstract

This study presents a modified algorithm for the inverse calculation of a multistage axial compressor using the established streamline curvature method. The algorithm was applied to design a four-stage axial compressor with a pressure ratio of 3.2 and an estimated efficiency of 88.6%. Numerical simulations of the designed compressor were performed, showing good agreement with the calculated values at the mean diameter, with deviations within 5%. The temperature distribution along the radial direction was predicted accurately, while some discrepancies in pressure prediction near the hub were observed due to the approximate nature of the loss models used. The study provides recommendations for improving the calculation methodology and confirms the reliability of the proposed modifications to the design method. These findings enhance the preliminary design process for axial compressors, contributing to their efficiency and reliability.

Keywords: Axial Compressor; Streamline Curvature Method; Inverse Solver; Preliminary Design.

1. INTRODUCTION

In modern gas turbines, the axial compressor is an essential part. Aerodynamic design and optimization need a thorough understanding of its flow characteristics and performance across a wide variety of operating situations. Three-dimensional computational fluid dynamics (CFD), the one-dimensional approach, and the through-flow method are the main computational techniques employed in compressor research. The one-dimensional approach skips the in-depth flow study in favor of concentrating on the general traits and functionality of the compressor stage [1].

The streamline curvature method is a standard tool used for the design and analysis of turbomachinery, particularly in the context of designing axial multistage machines. The use of the streamline curvature method as applied to analysis in multistage axial compressors was described by Jansen and Moffatt[2], Aungier [3], Campsty [4], and many other authors. Jansen and Moffatt [2] represent an early foundational study in the designing axial multistage machines. References [3] and [4] are relatively modern seminal texts that comprehensively detail

https://doi.org/10.61150/ijonfest.2024020204
Copyright © 2024 IJONFEST

axial multistage compressors' theory and design methodologies. Banjac [5] provided a reasonably detailed description of the design methodology using the streamline curvature method. Suppose the body and sleeve geometry are modified in that design throughout the calculation process. In that case, the only thing that changes in this work is the blades' edge positions, which will be covered in more detail below.

Existing methodologies [3,4] typically propose conducting the compressor calculation sequentially from section to section along its flow path. However, an appealing approach is the method of calculating parameters simultaneously considering all sections. This approach simplifies the computation of partial derivatives of compressor parameters and avoids nested loops in the calculation program. Nevertheless, this method has a drawback: ensuring the stability of the solution process becomes more challenging. When solving the inverse problem, the complexity increases because geometry updates of the compressor are required at each iteration, which can lead to computational instability.

It is vital to enhance inverse solvers made specifically for compressor design in order to enhance the features of axial compressors. Early-stage design solvers that consider a wide range of parameters influencing the machine's efficiency are required. Studying the inverse solver's algorithms, as well as the physical processes taking place in the compressor's flow section, are necessary to do this.

In compressor design, it is crucial to select loss models appropriately and consider parameters such as incidence angles, deviation angles, and blockage factors. For instance, inaccurately calculated losses or blockage factors may result in meridional velocity variations from the design values. This mismatch in compressor stage operation lowers the compressor's efficiency and surge margin. Improper distribution of losses along the blade height can result in insufficient performance near the casing, leading to flow degradation and boundary layer separation.

In this paper, we propose an original algorithm for the inverse calculation of multistage axial compressors. This algorithm addresses some of the challenges by updating only the position of the blade edges during the calculation process, which aims to enhance computational stability. The proposed algorithm has been applied to the design of a four-stage axial compressor, showing promising results that suggest its potential effectiveness.

2. MATERIAL AND METHODS

2.1 Radial equilibrium equation

The streamline curvature method is based on the radial equilibrium equation. This method does not take into account viscous effects and assumes an axisymmetric flow [4]. Figure 1 presents a fluid flow diagram in the meridional plane with the designation of the coordinate system.

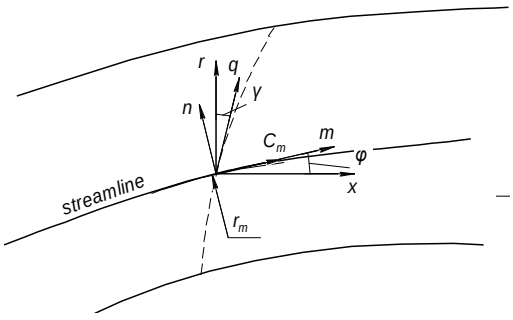

Figure 1. Coordinate system for streamline curvature method calculation

Copyright © 2024 IJONFEST

The equation is shown below in the generally recognized form [4], except that the term that accounts for blade forces in the radial direction is missing in this particular case. It is possible to ignore this term in the axial compressors.

$$\frac{1}{2}\frac{\partial}{\partial q}C_m^2 = \frac{\partial h_0}{\partial q} - T\frac{\partial s}{\partial q} + C_m\frac{\partial C_m}{\partial m}\sin(\phi+\gamma) - \frac{C_m^2}{r_m}\cos(\phi+\gamma) - \frac{1}{2r^2}\frac{\partial}{\partial q}\left(r^2C_u^2\right) \quad (1)$$

In this case, the variables are: ϕ is the angle between a stream-surface and the compressor axis; γ is the angle between the quasi-normal and the plane perpendicular to the compressor axis; C_m is the meridional velocity; C_u is the circumferential velocity; h_0 is the total enthalpy; and s is the entropy.

2.2 Calculation procedure

Upon completing the compressor calculation based on the mean diameter, the shape of its flow path is determined. Subsequently, a two-dimensional axisymmetric calculation is necessary to ascertain the flow kinematics along the blade height of the compressor. To achieve this, a computational grid is generated (Figure 2a) for further calculation based on the obtained geometry of the flow path. During the first iteration, the blade width is assumed to be constant along the height and equal to the value obtained from the mean-line calculation. The blade width depends on the chord of the blade and the stagger angle of the blade profile, which in turn is completely determined by the flow kinematics. Then, in each subsequent iteration, the blade width is refined for each section, and based on this refinement, the position of the nodes of the computational mesh is updated.

The calculation process is as follows:

1) Initially, the positions of the stream surfaces are estimated. Typically, they are arranged to divide the surfaces formed by the rotation of quasi-normals into surfaces of equal area.

2) Angles ϕ and the curvature of the stream surfaces r_m are determined at the intersection points with the quasi-normals. Then, by interpolation, the values of these parameters are determined at the grid nodes (Figure 2b).

3) Values of the angle γ are determined at the grid nodes.

4) In the initial approximation at the first iteration, the values of the meridional velocity C_m and entropy s are assumed constant with height, derived from mean-line calculation results. On each subsequent iteration, these values are taken from the calculation results of the previous iteration. A relaxation coefficient may be applied for calculation stabilization.

5) Values of the total enthalpy h_0 and velocity C_u are determined at each node. At the rotor inlet, C_u is determined based on the twist law, while at the rotor outlet, it is determined to ensure the required work at the given rotor radius.

6) Terms of equation 1 are evaluated at each point. Then, by integrating equation 1, updated values of C_m are determined for each point. The boundary condition for integrating the equation is taken as the value of velocity C_m at the mean diameter.

7) Using the new values of C_m, losses are evaluated for each blade section, and the entropy s is updated.

8) The flow rate through each quasi-normal is calculated, and the values of C_m are updated to ensure the specified flow rate through each quasi-normal. This may be accomplished by multiplying all of the C_m values in the current quasi-normal by a coefficient that is the same as the ratio of the specified flow rate to the calculated flow rate.

9) If necessary, the blockage factors are updated. Here, a relaxation coefficient may also be used to ensure calculation stability.

10) Blade width values are updated, and based on this, the position of grid nodes is updated.

11) The positions of the stream surfaces are updated to ensure flow continuity in each stream tube formed by adjacent stream surfaces.

12) Residuals are evaluated, and if necessary, the calculation is repeated from step 2.

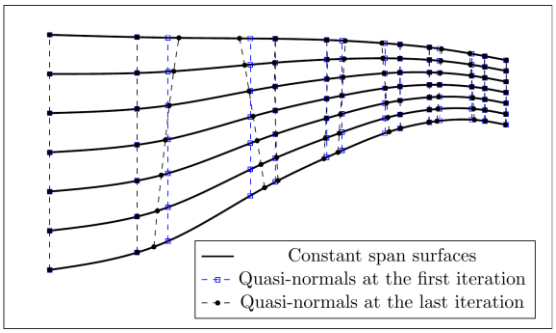

(a) Illustration of node position update

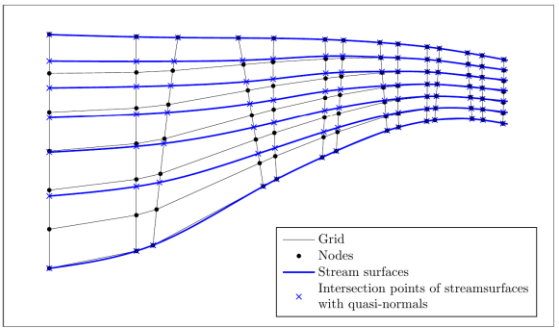

b) Illustration of intersection points between stream surfaces and quasi-normals

Figure 2. Computational grid

2.3 Loss Correlations

The loss coefficient is calculated from the drag coefficient, which in turn is composed of coefficients of resistance caused by various types of losses:

$$\bar{\omega} = C_D \sigma \frac{\cos^2 \beta_1}{\cos^3 \beta_m}$$

$$C_D = C_{Dp} + C_{Da} + C_{Ds} + C_{Dt}$$

where $\bar{\omega}$ is loss coefficient, C_D – total drag coefficient, C_{Dp} – drag coefficient from profile losses, C_{Da} – drag coefficient end-wall losses C_{Ds} – drag coefficient from secondary losses, C_{Dt} – drag coefficient from tip clearance losses, σ – row solidity at mean diameter, β_1 – inlet flow angle at relative frame, β_m – averaged flow angle which calculated as:

$$\beta_m = \arctan\left(\frac{\tan\beta_1 + \tan\beta_2}{2}\right)$$

where β_2 is the outlet flow angle at the relative frame.

Profile losses are estimated using the widely accepted Lieblein's model [6]:

$$C_{Dp} = 2\left(\frac{\theta_2}{l}\right)\left(\frac{\cos\beta_m}{\cos\beta_2}\right)^3\left(\frac{2H_2}{3H_2 - 1}\right)\left[1 - \left(\frac{\theta_2}{l}\right)\frac{\sigma H_2}{\cos\beta_2}\right]^{-3}$$

where β_m – averaged flow angle at the relative frame, β_2 – outlet flow angle at the relative frame, σ – row solidity at mean diameter, H_2 – boundary layer shape factor, θ_2 – blade wake momentum thickness, c – blade chord.

The prediction of endwall losses and secondary losses is based on the Howell model [7]:

Copyright © 2024 IJONFEST

$$C_{Da} = 0.02\frac{s}{H}$$

$$C_{Ds} = 0.018C_L^2$$

where s is blade pitch, H – blade height, C_L – lift coefficient.

An empirical model has been used to estimate losses from leakage in the radial gap:

$$C_{Dt} = 0.29\bar{t}C_L^{1.5}$$

here $\bar{t}$ is the relative tip gap, C_L – lift coefficient.

The lift coefficient is calculated as:

$$C_L = \frac{2}{\sigma}\left(\tan\beta_1 - \tan\beta_2\right)\cos\beta_m$$

where σ is row solidity at mean diameter β_1 – inlet flow angle at relative frame, β_2 – outlet flow angle at relative frame, β_m – averaged flow angle.

2.4 Designed compressor parameters

The main parameters of the designed compressor are given in Table 1. The compressor is a four-stage compressor with a pressure ratio of 3.2. At this pressure ratio, the compressor stages are usually lightly loaded and usually provide fairly high efficiency. Based on one-dimensional calculations, the estimated efficiency is 88.6%. The air mass flow rate is 50 kg/s, which corresponds to a medium-sized compressor. The relative hub diameter in the first stage is 0.5, which provides a balance between compressor performance and acceptable efficiency.

Table 1. Compressor main parameters

Parameter	Unit	Value
Number of stages	[-]	4
Mass flow rate	[kg/s]	50
Pressure Ratio	[-]	3.2
Isentropic Efficiency	[-]	0.886
Shaft Speed	[RPM]	9550
Inlet Hub-Tip Ratio	[-]	0.5

Figure 3 shows the meridional cross-section of the compressor flow path. During the calculation, the end diameter was chosen as the determining one, and this diameter decreased by 4% from the compressor inlet to the outlet.

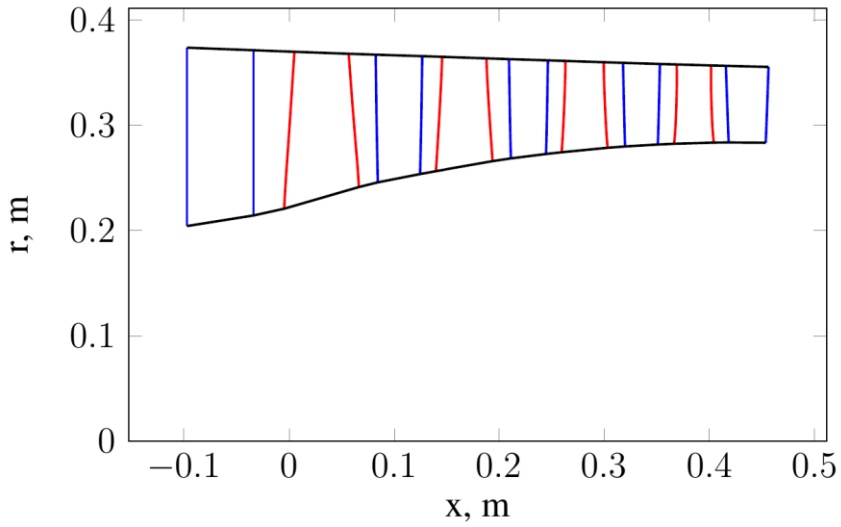

Figure 3. Compressor flow path

Table 2 presents the main parameters of the compressor stages. Figure 4 shows the distribution of pressure ratio, isentropic efficiency of the compressor stages and the equivalent diffusion factor of the compressor rows.

The flow coefficients were selected from values from 0.5 to 0.59. These values provide an axial velocity of 174.6 m/s at the entrance to the first stage rotor and 160 m/s at the exit from the compressor. The outlet flow angles in the stators of the first and second stages are 16 degrees, which ensures an acceptable degree of reaction and, accordingly, increased efficiency of the stages. At the third stage, this angle is 12 degrees, which makes it possible to achieve acceptable efficiency values and, at the same time, reduce the load on the final stage stator by decreasing the flow angle behind the final stage rotor.

Table 2. The compressor stage's main parameters

	Unit	IGV	1st stage	2nd stage	3rd stage	4th stage
Blade speed at mean diameter	[m/s]	-	296	310.4	317.5	320.1
Blade corrected speed at mean diameter	[m/s]	-	296	292.3	284.4	275.4
Total temperature rise	[K]	-	36.6	34.4	30	26.3
Axial velocity at the inlet	[m/s]	149.2	174.6	172.2	168.3	160
Work coefficient	[-]	-	0.42	0.36	0.3	0.26
Flow coefficient	[-]	-	0.59	0.555	0.53	0.5
Stator outlet flow angle	[°]	12	16	16	12	2
Rotor de-Haller Number	[-]	-	0.709	0.727	0.749	0.765
Stator de-Haller Number	[-]	1.196	0.787	0.764	0.764	0.767

Copyright © 2024 IJONFEST

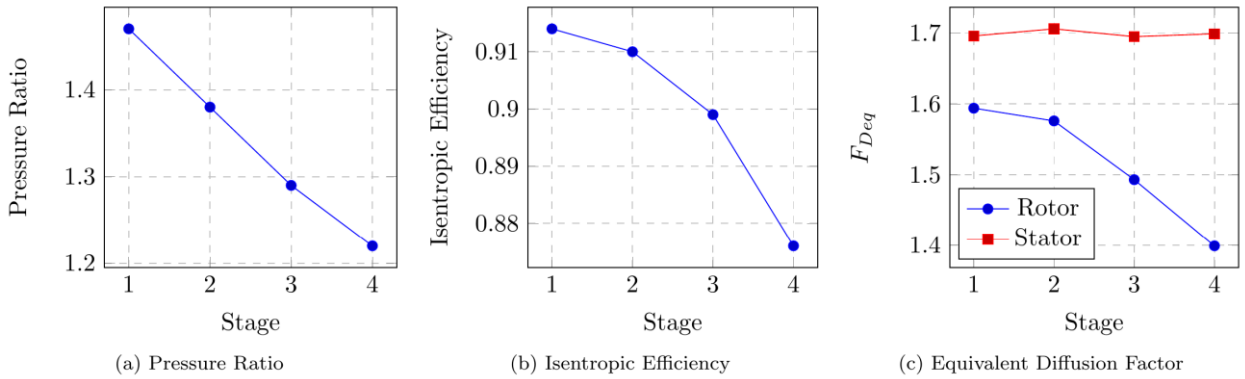

Figure 4. Stages parameters

Work coefficients were also selected to ensure high-stage efficiencies but were adjusted to limit the aerodynamic loading of the stators to $F_{Deq}=1.7$. Since the stators of the third and fourth stages have to correct the flow, swirled in the first two stages, their aerodynamic load increases, so the rotors of these stages are underloaded. Accordingly, if the temperature increased by 36.6 and 34.4 degrees in the first two stages, respectively, in the third stage, it will climb by 30 degrees and by just 26.3 degrees in the second stage.

The speed of the blades at the mean diameter is moderate, from 296 to 320 m/s, which makes it possible to manufacture the compressor rotor from inexpensive materials. The corrected blade speed at the mean diameter varies from 296 m/s at the inlet to 275.4 m/s at the outlet. These values correspond to transonic stages.

2.5 CFD modeling

Based on the results of aerodynamic calculations, the compressor blades were profiled, and a 3D model of the aerodynamic surfaces was created. DCA profiles were used for the rotor blades and IGV blades, and NACA65 profiles [7] were used for the stator blades. The resulting 3D model is shown in Figure 5.

The Ansys CFX [9] software package was used for the numerical simulation of the flow in the compressor. This package allows for the calculation of RANS (Reynolds-Averaged Navier-Stokes) equations using the finite volume method.

A high-quality hexahedral mesh was generated in TurboGrid. The number of elements per row ranged from 0.5 to 2.0 million. Near the walls, the mesh was refined so that the thickness of the first element was between 3 and 5 microns, ensuring y+ values of less than 5. A radial clearance of 0.5 mm was implemented on the rotor blades. Figure 6 shows the resulting mesh. The total number of elements was 9.2 million, and the number of nodes was 9.54 million.

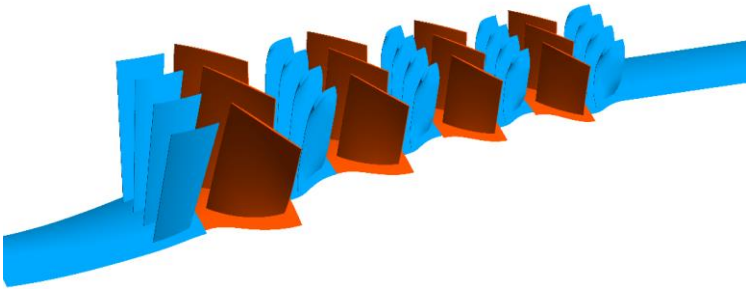

Figure 5. 3D model of the designed compressor

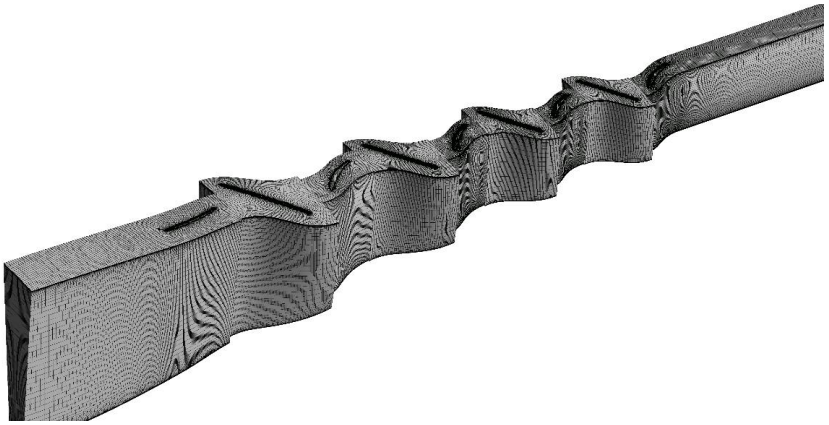

Figure 6. Computational mesh

The full energy model is used in the simulation. The turbulence model is SST. A periodic boundary condition allows the calculation to consider only one interblade passage. The boundary condition for the walls is a no-slip condition. At the inlet, the total pressure is set to 101.325 kPa and the total temperature to 288.15 K, while the outlet has an average static pressure of 290 kPa. The rotation speed of the computational domain is set to 9550 RPM. The convergence criterion is that the root mean square residuals reach a level of 1e-4.

3. RESULTS AND DISCUSSION

Table 3 presents the integral parameters of the compressor obtained as a result of numerical simulation in comparison with the design values. Despite the blockage coefficients taken into account during the design, the flow deficit was 3.6%, which is likely due to incorrect calculation of the channel blockage and incorrectly selected angles of attack in the rotor of the first stage of the compressor. The shortfall in efficiency was 1.6%, which is not much for preliminary design. The deviation of the pressure ratio from the design value was -2.81%.

Table 3. Integral Parameters

	Unit	Design	CFD	Rel. diff.
Mass Flow	[kg/s]	50.0	48.2	-3.60%
Isentropic efficiency	[-]	0.886	0.870	-1.81%
Pressure ratio	[-]	3.20	3.11	-2.81%

In Figure 7, the calculation results for the hub, middle and tip sections of the compressor are presented in the form

Copyright © 2024 IJONFEST

of Mach number fields and vector fields. From these figures it is clear that in the middle and end sections the flow proceeds without areas of developed boundary layer separation, while in the hub section there are areas with intense boundary layer separation in the stator rows. It can also be noted that there are areas with pronounced shock waves in the first stage rotor, where the temperature is the lowest.

The graphs (Figure 8) illustrating the distribution of total pressure and temperature indicate that in the first stage, above the mean diameter, the work performed exceeds the design specifications. Further, in the second and third stages, the pressure curve somewhat levels out in the flow core, while at the core of the blades there are strong dips in the total pressure due to the presence of boundary layer separation in these zones. In the fourth stage, the total pressure over the entire height is below the design value. It should be noted that there is a drop in total pressure already behind the first stage, which can cause degradation of the flow in the area of the end-walls and, therefore, a rapid increase in the thickness of the boundary layer and its separation [10].

Regarding the distribution of the total temperature, it should be noted that in all stages there is approximately the same difference from the design values in the area of the end walls, which is probably caused by mixing processes in the boundary layer, which were not taken into account during the design. The entropy distribution graphs show that there is an approximately constant difference with the design values, which indicates that the design did not take into account the uneven distribution of entropy at the entrance to the compressor, which could also cause degradation of the flow near the end walls further along the compressor flow path.

During the design process, it is essential to highlight that the distribution of losses with respect to height was somewhat inaccurate. In the event where the design of the entropy distribution curves is supposed to be parabolic, the modeling results show discrete linear portions in the entropy distribution curves for the initial three stages. However, in the final stage, characterized by enhanced mixing, the curve is notably smoothed and closely approximates the originally intended design shape.

Figure 9 shows graphs of the distribution of flow angles at the inlet and outlet for each row of the compressor, and Figure 10 shows graphs of the distribution of meridional velocity. It is evident from Figure 9a that the rotor's angle of attack was set wrong, which resulted in inadequate flow through the compressor. Judging by the other figures, this may also be true for the rotors of subsequent stages. To increase flow rate, it is recommended to increase the angles of attack for rotor cascades. If the stators of the first three stages level the flow over most of the blade height, while due to the intense separation of the boundary layer, the stator of the last stage provides kinematic flow parameters close to the design ones only in the flow core.

The meridional velocity distribution graphs demonstrate that there was a notable departure from the design values of the meridional velocity as early as the first stage entry. This divergence was most noticeable in the vicinity of the hub wall. This effect only increases further along the compressor flow path. This deviation from the design parameters could also cause increased losses at the bushing and, as a result, degradation of the flow closer to the compressor outlet.

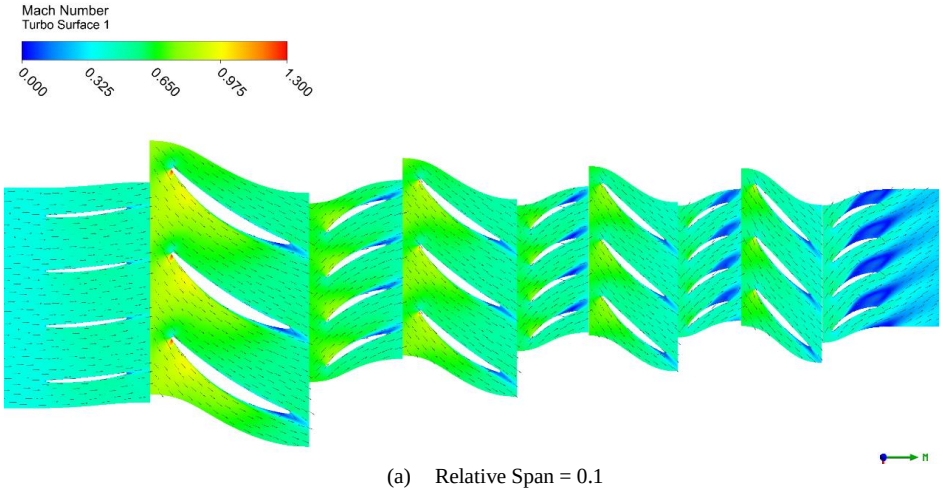

(a) Relative Span = 0.1

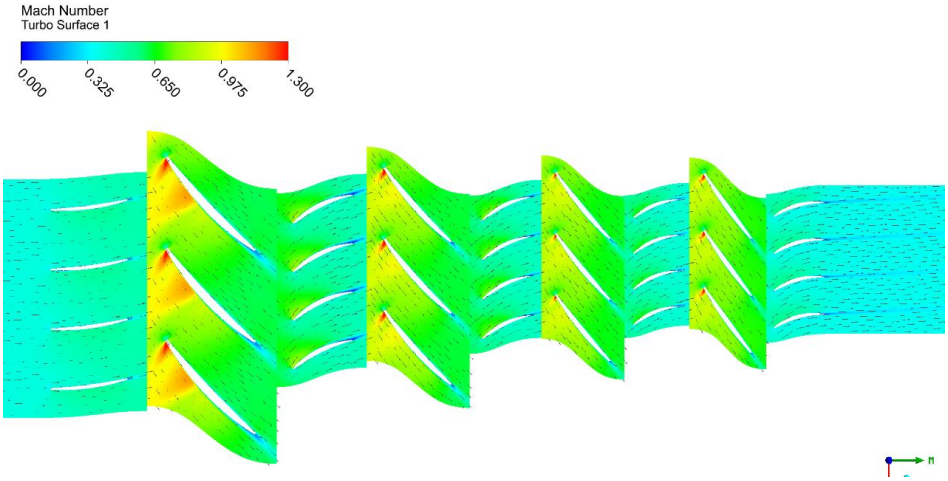

(b) Relative Span = 0.5

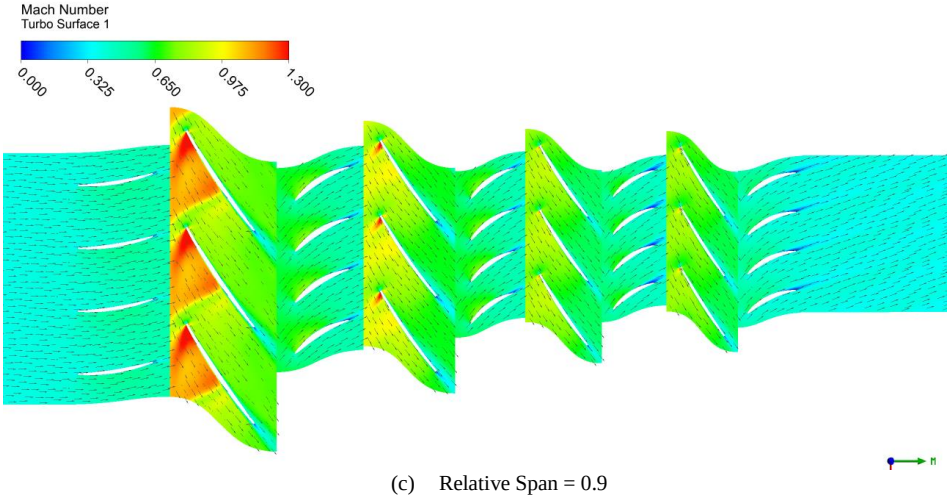

(c) Relative Span = 0.9

Figure 7. Mach number fields and vector fields

Copyright © 2024 IJONFEST

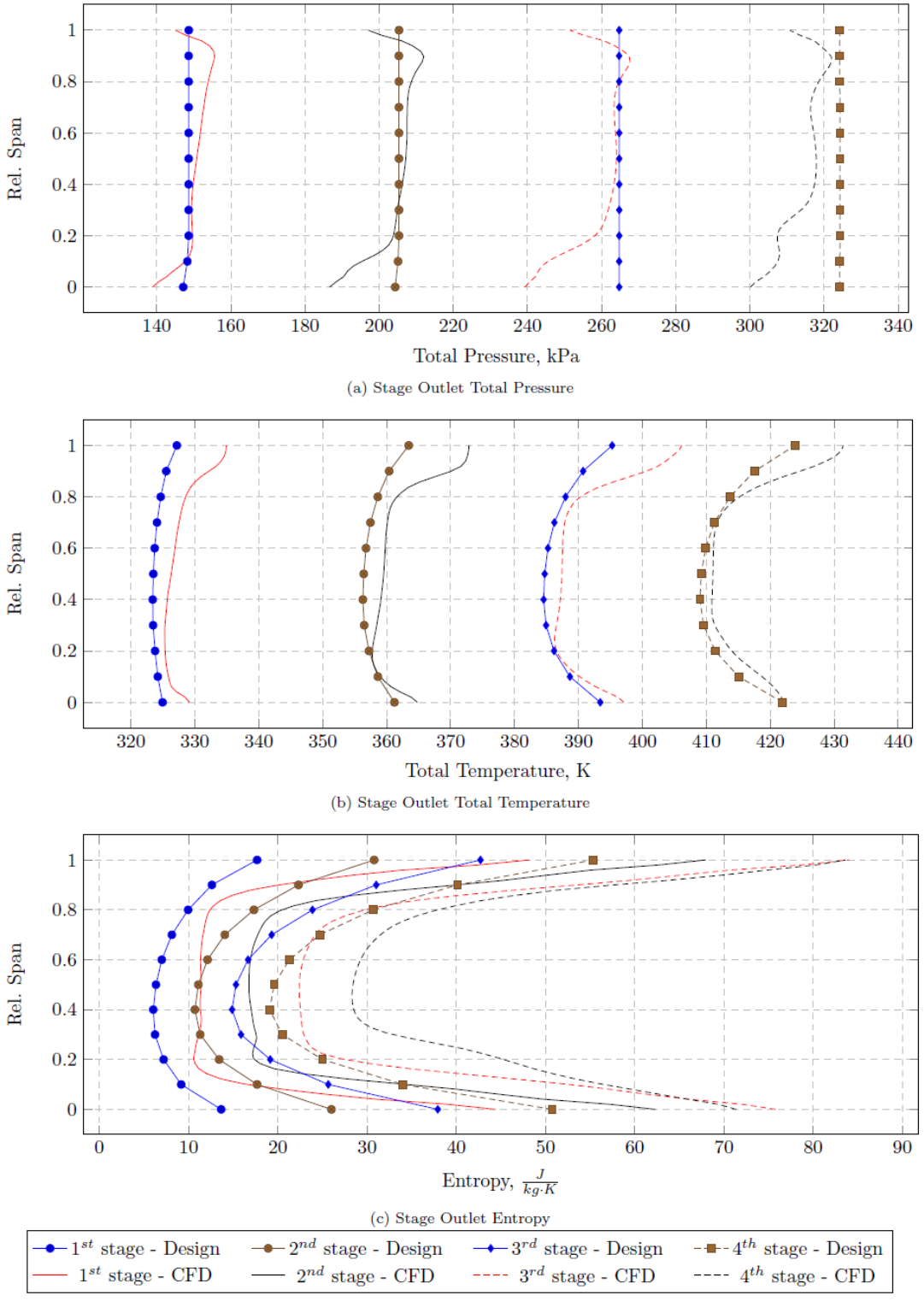

(a) Stage Outlet Total Pressure

(b) Stage Outlet Total Temperature

(c) Stage Outlet Entropy

Figure 8. Thermodynamic parameters

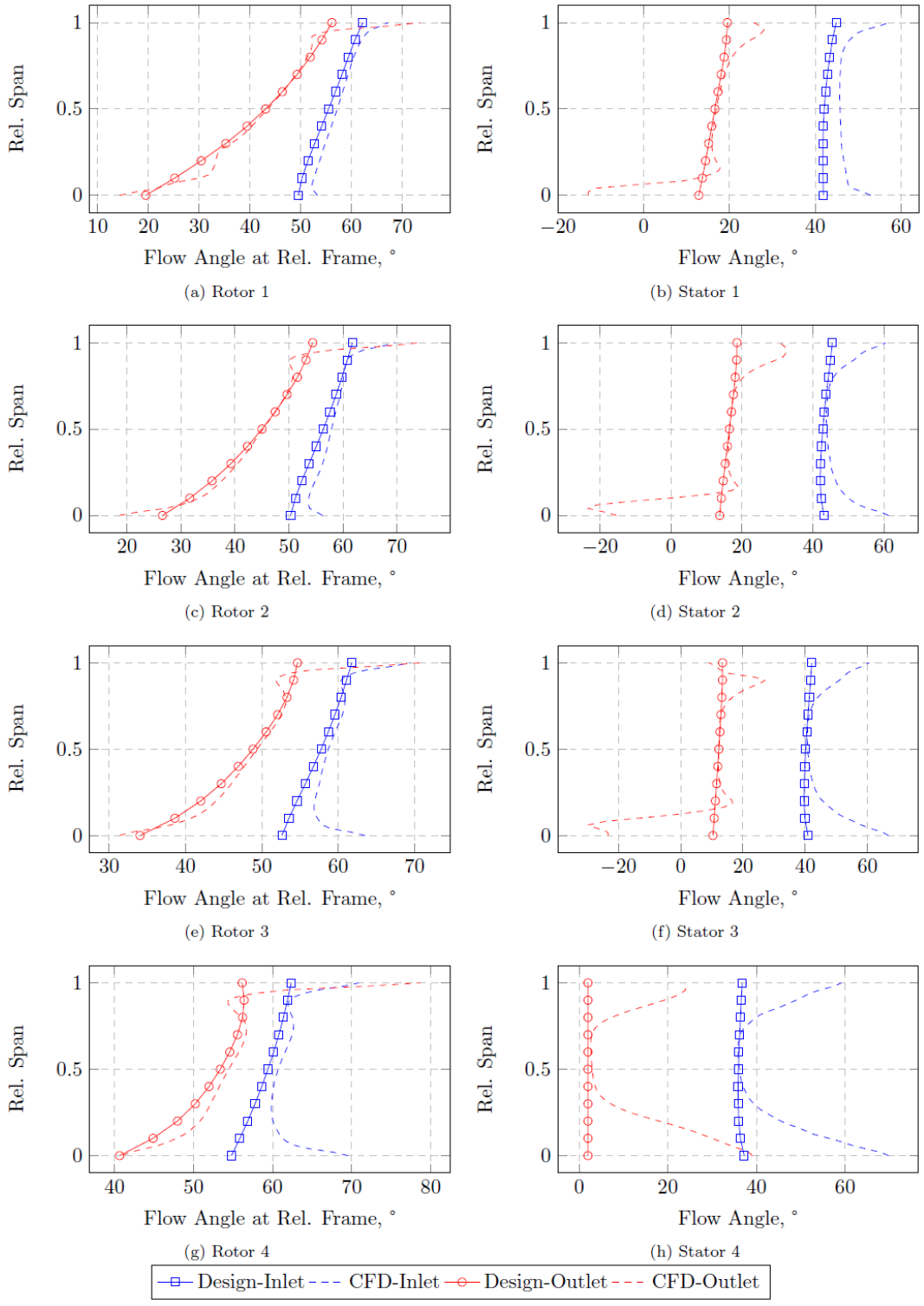

Figure 9. Flow angles

Copyright © 2024 IJONFEST

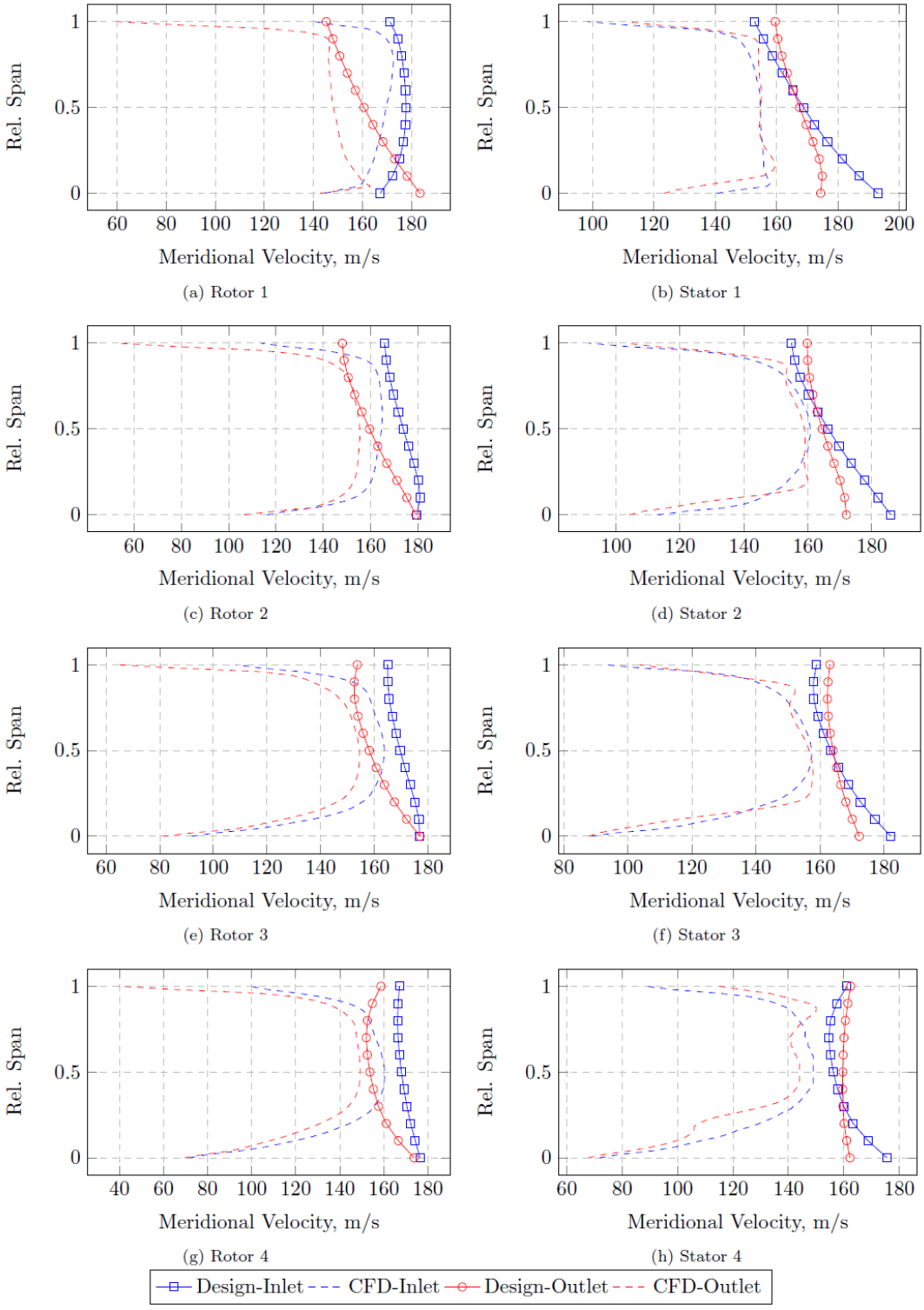

Figure 10. Meridional velocity

4. CONCLUSION

This study focused on the development and application of an inverse calculation algorithm specifically designed for the design of multistage axial compressors. The main task was to develop a four-stage axial compressor with a pressure ratio of 3.2

We proposed an inverse calculation algorithm to determine the geometric and aerodynamic parameters of multistage axial compressors based on specified target parameters. The algorithm was applied in the design of a four-stage axial compressor. Comprehensive numerical simulations were carried out to evaluate the performance of the designed compressor. This simulation provided a detailed understanding of the flow pattern and overall compressor efficiency. Numerical modeling results showed deviations from the design values: the mass flow rate deviation was -3.6%, the pressure ratio deviation was -2.81%, and the isentropic efficiency deviation was -1.81%.

Additionally, there were local deviations in the thermodynamic and kinematic parameters from the design values caused by the following reasons:

- Inaccurate estimation of channel blockage.
- Incorrectly selected incidence angles in the compressor rotors.
- Improper distribution of losses along the blade height.

These factors led to flow degradation along the compressor's flow path, resulting in boundary layer separation from the hub surface.

Despite these issues, the developed software code allows for the preliminary design of a compressor with parameters close to the design values. However, to improve the program, the following recommendations are made:

- Advanced Channel Blockage Prediction: Use more advanced methods for predicting channel blockage, such as calculating the boundary layer on the end walls of the compressor.
- Enhanced Loss Models: Employ more sophisticated loss models, particularly regarding their distribution along the blade height. This could involve implementing three-dimensional loss models that account for secondary flows and other complex phenomena.
- Meticulous Angle of Attack Selection: Conduct a more meticulous selection of angles of attack. This can be achieved through more precise optimization algorithms and taking into account the variable flow conditions across different stages.
- Consider Blade Height Mixing: It is recommended to take into account blade height mixing, which is especially important for compressors with more than 3-4 stages. This consideration can help accurately predict and mitigate adverse flow effects.

By implementing these recommendations, the accuracy and reliability of the compressor design process can be significantly improved, resulting in higher efficiency and better overall performance.

Future research will focus on calibrating loss models and accurately distributing these losses along the blade height. Additionally, the calculation of the boundary layer on the end walls of the compressor will be a key area of study to better estimate flow path blockage. Furthermore, modifications will be made to the computational code to account for mixing effects, which is essential for the accurate design and analysis of multistage compressors.

Copyright © 2024 IJONFEST

References

[1] Tao, L., Yadong, W., & Hua, O. (2020). Performance Prediction of Transonic Axial Compressors Using Improved Streamline Curvature Approach. Fluid Dynamics, 55(1), 121–132.
[2] Jansen, W., & Moffatt, W. C. (1967). The off-design analysis of axial-flow compressors.
[3] Aungier, R. H. (2003). Axial-flow compressors. American Society of Mechanical Engineers, New York.
[4] Cumpsty, N. A. (1989). Compressor aerodynamics. Longman Scientific & Technical.
[5] Banjac, Milan & Petrovic, Milan. (2018). Development of Method and Computer Program for Multistage Axial Compressor Design: Part II — Two-Dimensional Design and Validation Using CFD. V02CT42A008. 10.1115/GT2018-75412.
[6] Lieblein, S., 1959. “Loss and Stall Analysis of Compressor Cascades”. ASME Journal of Basic Engineering, 81, pp. 387–400.
[7] Schobeiri, M. (2005). Turbomachinery flow physics and dynamic performance (p. 153). Berlin: Springer.
[8] Bogdonoff, S. M. (1948). NACA Cascade Data for the Blade Design of High-Performance Axial-Flow Compressors. Journal of the Aeronautical Sciences, 15(2), 89-95.
[9] ANSYS, 2010. ANSYS CFX-Solver Theory Guide. ANSYS Inc, Canonsburg.
[10] Statrtsev, A.N. (2021). Аэродинамическое проектирование осевого компрессора [Design of an axial compressor aerodynamics]. Aircraft Engines 3(12), 19-34.